A Mimicking Enzyme Analogue for Chemical Sensors

JYH-MYNG ZEN* AND
ANNAMALAI SENTHIL KUMAR
Department of Chemistry, National Chung-Hsing University, Taichung 402, Taiwan

Received August 8, 2000

ABSTRACT
An artificial enzyme analogue of Nafion/lead−ruthenium oxide pyrochlore (Py) chemically modified electrode (NPyCME) is synthesized by in situ precipitation through blocking of Nafion's hydrophilic zones. The catalytically active Py sites covered with a hydrophobic core of Nafion resemble an enzymatic structure. Moreover, the NPyCME obeys the Michaelis−Menten mechanism for the oxidation of many organic and biological molecules. This Account highlights aspects of the preparation, characterization, and application of the NPyCME.

Introduction

The development of chemical sensors through electrocatalysis for detection and determination of various organic and biomolecules has potential implications for clinical, biomedical, and environmental research fields. Precious metallic oxides, namely PtO_2, IrO_2, and RuO_2, usually have fascinating and excellent electrocatalytic activity over simple mediator systems.[1] This is because these oxides contain tunable redox groups with large specific surface area. A successful chemical sensor must have good sensitivity, selectivity, reversibility, speed, and longevity toward the desired analyte while consuming minimal power and volume; additionally, it must be able to be manufactured from inexpensive materials using economical batch methods.[2] Undoubtedly, the precious metallic oxide electrodes can fulfill only part of those requirements. Indeed, higher cost, long and high-temperature preparation, and large intrinsic capacitative behavior of these metallic oxides limit their utility in sensor applications. Conversely, mixed oxides derived from spinel, perovskite, and pyrochlore also showed good catalytic activity but at a much lower cost. Pyrochlores with general formula $A_2B_2O_6O'$ (where A = Pb, Bi, etc. and B = Ru, Ir, etc.) are especially anticipated to be a very good alternative for precious metallic oxides.[3,4] Lead−ruthenium oxide pyrochlore ($Pb_2Ru_2O_6O'$, Scheme 1) and lead−iridium oxide pyrochlore ($Pb_2Ir_2O_7$) have been reported as active bifunctional catalysts for both oxidation and reduction reactions.[1,3,4] Other pyrochlores, like $Bi_2Ru_2O_7$ and $Bi_2Ir_2O_7$, also have high conductivity and activity. However, these compounds have yet to be proved useful for electrocatalytic applications.

Scheme 1. (a) One-Quarter Cationic Sublattice of Lead−Ruthenium Oxide Pyrochlore (Py, $Pb_2Ru_2O_6O'$) Having Face-Centered Cubic Unit Cell, and (b) Illustration of Intact $RuO_{6/2}$ Octahedral Sites in the Py

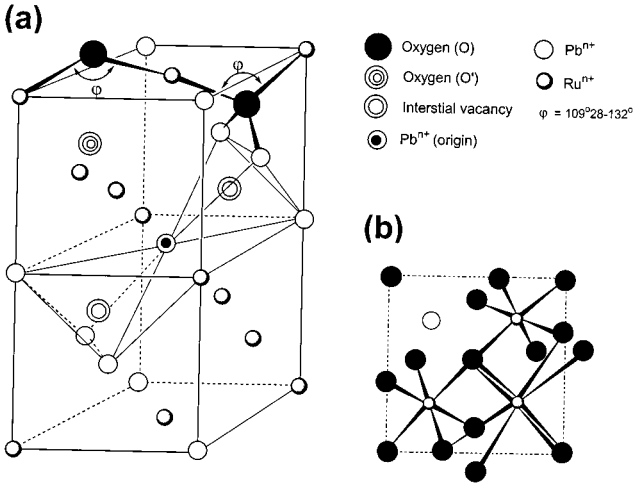

For utilization of the oxide materials in chemical sensor applications, the main requirement is to find a suitable modifier (or binder) and electrode modification procedures to convert the oxide material into an electrode. We disclosed earlier a novel Nafion/lead−ruthenium oxide pyrochlore chemically modified electrode (NPyCME) for chemical sensor applications, where the catalytically active pyrochlore (Py) units were directly precipitated in the interfacial sites of the Nafion matrix.[5,6] This electrode has a unique structure of hydrophobic core intercalated with active Py sites and is similar to an enzymatic structure. Compared parallel experiments under identical conditions with a Nafion (4 wt %) + Py (∼1.5 μg/cm^2) composite electrode (designated as NPyCE), the NPyCME shows a much smaller ionic and double-layer charging current and more efficient electrocatalytic action. The very low residual double-layer charging together with fast response time make the NPyCME further suited for the construction of good chemical sensors with detection limits in the nanomolar range.[5] Analytical applications were demonstrated with good sensitivity and selectivity for many samples, including those from the environmental,[5−8] biomedical,[9−14] and pharmaceutical and food[14−18] industries, through the NPyCME's electrocatalytic activity.

The electrocatalytic oxidation on the NPyCME obeys Michaelis−Menten (MM) type kinetics, as demonstrated

Jyh-Myng Zen was born in Taipei, Taiwan, in 1957. He obtained his B.S. degree in chemistry from National Tsing Hua University, Taiwan, in 1980. He served in the military 1980−1982. He studied electrochemistry with Larry R. Faulkner at University of Illinois, Urbana−Champaign, and graduated with a Ph.D. in 1988. For the next three years, he was a postdoctoral researcher with Allen J. Bard and John B. Goodenough, first in the Chemistry Department and later at the Center for Material Science and Engineering at the University of Texas−Austin. He is currently a professor in the Department of Chemistry, National Chung-Hsing Univeristy (NCHU), Taiwan. His research interests include chemically modified electrodes, electrocatalysis, photoelectrochemistry, physical electrochemistry, and chemical sensors.

Annamalai Senthil Kumar was born in Vellore, India (Tamilnadu) in 1968. In 1990, he received is master degree from the University of Madras, India, and he took educational training in 1991−1992 and obtained a Ph.D. (2000) in the Department of Physical Chemistry, University of Madras, under Prof. K. Chandrasekara Pillai in the field of ruthenium dioxide electrochemistry. He is currently a postdoctoral fellow in Prof. J.-M. Zen's laboratory. He is interested in polymer-modified metal oxide electrodes, electrocatalysis, and chemical sensors.

* Corresponding author. Fax: 886-4-22862547. E-mail: jmzen@dragon.nchu.edu.tw.

10.1021/ar000073n CCC: $20.00
Published on Web 09/27/2001

Scheme 2. Preparation Route for the Nafion/Lead-Ruthenium Oxide Pyrochlore Chemically Modified Electrode (NPyCME) by in Situ Precipitation Technique

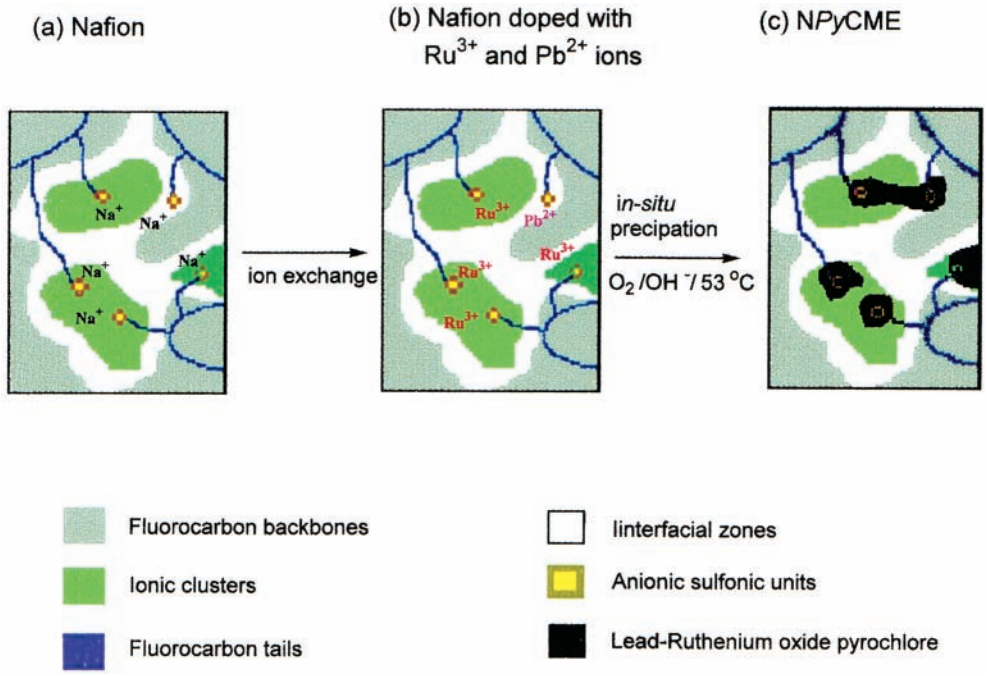

by quasi-steady-state cyclic voltammetric (CV) studies of cysteine, amitrole, hypoxanthine (Hx), etc.[8,13,14] The NPyCME actually behaves like an *enzyme analogue* similar to one predicted for catalytic reaction from an enzyme in a biological system.[19] Most importantly, the NPyCME fulfills the majority of the requirements in sensor applications. In this Account, we address the preparation and characterization of the NPyCME together with the mechanistic details of its electrocatalytic reaction.

In Situ Precipitation of Lead−Ruthenium Oxide Pyrochlore in Nafion Matrix

Scheme 2a represents the basic microstructural units of the Nafion-coated glassy carbon electrode (GCE), in which fluorocarbon backbones, ionic hydrophilic clusters (~15% water), and interfacial amorphous hydrophobic zones of lower ionic content coexist.[20] To prepare the NPyCME, the Nafion-coated GCE is first dipped into a solution of Pb^{2+}:Ru^{3+} (1.5:1) for ~12 h. Due to the difference in charge density and hydration energy between Ru^{3+} and Pb^{2+} ions, it is expected that the majority of the Ru^{3+} ions can get into ionic zones and Pb^{2+} into the interfacial zones. After the ion-exchange process, the electrode is taken out and washed to remove the loosely adsorbed cations. This is followed by cooking in alkaline solution with continuous purging of oxygen, as suggested by Horowitz et al., at a bath temperature of 53 °C.[21] After cooking for at least 1 day, the electrode becomes blackish due to the in situ precipitation of Py units (Scheme 2c). As indicated in Table 1, X-ray diffraction patterns of the NPyCME show a diffused crystalline pattern with face-centered cubic unit cells (Scheme 1), which is very similar to the results found with the powder samples.[22] This result confirms the formation of finite and active-crystalline catalysts in the interfacial sites of Nafion.

Table 1. X-ray Diffraction Data of Four Major Peaks for Lead−Ruthenium Oxide Pyrochlore ($Pb_2Ru_2O_6O'$) Particles[22] and for Those Synthesized in Nafion Matrix

		2θ	
hkl	*d*/Å	Py[22]	NPyCME
(222)	3.02	29.5	30.0
(622)	1.57	58.0	59.2
(440)	1.84	49.5	49.9
(400)	2.60	34.0	34.8

Electron-Transfer Reaction with Benchmark Model Systems

Since the anionic Nafion backbone is anticipated to be occupied by Py, it is necessary to characterize the NPyCME by using standard benchmark systems of anionic $Fe(CN)_6^{3-/4-}$ and cationic $Ru(bpy)_3^{2+/3+}$ redox complexes. As shown in Figure 1, the CV response of the NPyCME with 5 mM $Fe(CN)_6^{3-}$ has perfectly reversible behavior, similar to that observed on solid metal electrodes.[23] The peak potential is fairly close to that at a GCE, except that the current value is notably higher (~20%). Parallel experiments under identical conditions with the NPyCE show an obviously poorer response due to the strong electrostatic repulsion force between Nafion and $Fe(CN)_6^{3-}$. This observation reveals the diminishing of Nafion's anionic surface charge upon in situ precipitation of Py crystallites, which is regarded as a unique characteristic of the NPyCME over other ionomer-modified systems.

The CV experiments are also extended to the $Ru(bpy)_3^{2+}$ cationic system to evaluate the internal electrostatic interaction effect on the NPyCME. As shown in Figure 1b,

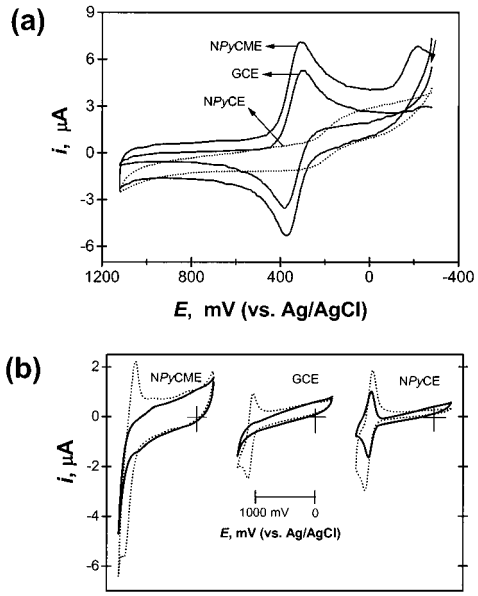

FIGURE 1. Electron-transfer reaction with benchmark model systems in pH 7.4 buffer ($I = 0.1$ M). (a) CV responses at different modified electrodes with 5 mM $Fe(CN)_6^{3-/4-}$ ($v = 10$ mV/s). (b) CV responses in 1 mM $Ru(bpy)_3^{2+/3+}$ before (dashed line) and after (solid line) transfer to the pure base electrolyte solution ($v = 50$ mV/s).

all three electrodes show well-defined peaks at 1100 mV vs Ag/AgCl, corresponding to the $Ru(bpy)_3^{2+/3+}$ redox transitions. To understand whether the electron-transfer process of $Ru(bpy)_3^{2+}$ is adsorption- or diffusion-controlled, the NPyCME is washed gently in distilled water and then transferred to the pure base electrolyte solution after experiments with $Ru(bpy)_3^{2+/3+}$. As shown by the solid line of Figure 1b, it is clear that there is no adsorption behavior on both the NPyCME and GCE, while for the NPyCE, the adsorption effect dominates due to the anionic character of Nafion. These results clearly show that the NPyCME surface is free from specific ionic charge effects, and its behavior is similar to that of a solid metal electrode.

Mechanistic experiments with $Fe(CN)_6^{3-}$ at different pH values also show similar metallic behaviors. The peak potential separation (ΔE_p) lies in the range of 80 ± 5 mV for the pH window of 1−13 at a scan rate of 10 mV/s. The ΔE_p is about 100 mV at 200 mV/s, indicating the quasi-reversible nature of the NPyCME. Similar observations have already been repported for Pt and Au electrodes in the pH range of 4−9.[23] Nevertheless, the facts that the anodic to cathodic peak current ratio (i_{pa}/i_{pc}) is close to 1 over the entire pH range and that the current function is independent of pH indicate a nearly ideal behavior. Heterogeneous electron-transfer rate constants (k^o) are calculated on the basis of the Nicholson model for a quasi-reversible system using the equation $k^o = \psi[D_o\pi\nu nF/(RT)]^{1/2}(D_R/D_o)^{\alpha/2}$, where ψ is the kinetic parameter that relates to ΔE_p and other symbols have their usual meaning.[24] The obtained k^o values are also independent of pH, with an average value of $(2.9 \pm 1.5) \times 10^{-3}$ cm/s. Compared to the earlier reported k^o values of $(2-6) \times 10^{-3}$ cm/s (GCE in 0.5 M K_2SO_4), $(2.0 \pm 1.5) \times 10^{-3}$ cm/s (Pt in 0.1 M LiCl), and $(1.1-38.8) \times 10^{-3}$ cm/s (Pt in 1 M KNO_3),[23,25−27] the similarity to the standard solid electrodes again demonstrates the near ideality of the present system.

The formal redox potential ($E^{o\prime}$) on the NPyCME is likewise independent of pH over the range 4−13, whereas a decreasing trend (~150 mV) is noticed between pH 2 and 4. This variation is not electrode-sensitive because the same decreasing trend was also noticed on Pt and Au electrodes due to the protonation effect of $Fe(CN)_6^{4-}$ ($pK_a < 3$ in 0.5 M K_2SO_4).[23,28] Note that the $Fe(CN)_6^{3-/4-}$ redox system shows a strong pH dependency on a GCE because the carbonyl functional groups on GCE exhibit a tremendous influence on the electron-transfer kinetics.[23] This phenomenon is, indeed, an additional advantage of the NPyCME, as it can be applied in a broad range of pH and potential windows in electroanalytical applications. From these observations, it is expected that the electron density is high enough to prevent a detectable potential drop across the surface layer. This result is substantially in agreement with ac-impedance conductivity measurement of the NPyCME. The potential drops by about 3 orders of magnitude after in situ precipitation of Py units in Nafion.[29] Overall, the general behavior of the NPyCME is typically metallic, similar to that reported on thermally prepared RuO_2 samples.[1]

Electrocatalysis and Mechanistic Aspects on the NPyCME

The electrocatalytic processes on the NPyCME occur through mediation by a higher oxidation state of $-Pb^{n+}$ or $-Ru^{n+}$ in the Py molecules. Basic studies revealed that $n = 4$ and $n = 7$ are the maximum values for $-Pb^{n+}$ and $-Ru^{n+}$, respectively.[1] With regard to the electrochemical behavior of Py, Goodenough et al. reported that the major electrochemical contribution is from octahedral Ru^{n+} in the $RuO_{6/2}$ framework.[3] Moreover, based on the Ru redox transitions of RuO_2, i.e., $Ru^{III/IV}$ (~0.4 to 0.5 V vs RHE), $Ru^{IV/VI}$ (~0.9 to 1.15 V vs RHE), and $Ru^{VI/VII}$ (~1.35 to 1.45 V vs RHE, only available at pH > 12),[1,30−32] the organic compound oxidation reactions investigated all lie in the reported redox potential windows.[33] For example, the starting oxidation potential of 0.26 V vs Ag/AgCl at pH 7.0 (i.e., 1.026 V vs RHE) for cysteine falls exactly in the potential window of 0.9−1.15 V vs RHE, and the reaction can therefore be regarded as being mediated by the $Ru^{IV/VI}$ redox couple.[13,29] In addition, our recent electrochemical and redox behavior comparison study of RuO_2 and Py powder modified polymer composite electrodes confirmed the predominant participation of the higher oxidation Ru^{n+} species.[34]

It was reported earlier that, with the reversible redox couple ($Fe^{2+/3+}$), the activation energy ($\Delta H^{\#}$) is low (~24 ± 2 kJ/mol) and independent of substrate (Pt or RuO_2), indicating a simple *outersphere* electron-transfer reaction on the electrodes.[35] Since there is no specific alteration in the formal potentials of the benchmark model systems on the NPyCME and GCE, the catalytic mechanism is unlikely to follow the above model systems. Note that

Table 2. Mechanistic and Analytical Data for Various Organic and Biochemical Compounds on the NPyCME

			against GCE				Michaelis−Menten parameters			
sample	pH	E_{pa}/mV	η/mV	I_{mag}	i_f /AV$^{-1/2}$ s$^{1/2}$ mol^{-1} cm^3 [a]	$C_L/\mu M$ [b]	K_m/mmol dm^{-3}	k_c/s^{-1}	D_L (μM)/technique	assayed real samples
oxygen	2.0	−500	250	+5.2					0.7−8.4 ppm/SWV	dissolved oxygen[6]
hydrazine	8.0	600	v. high	v. high	86.9	769	4.381	0.477	0.15/FIA[7]	
amitrole	3.6	910	v. high	v. high	256.2	400	0.310	0.189	0.38/SWV[8]	
acetaminophen	1.7	700	100	+8.2	191.6	12300	53.100	9.020	1.2/SWV	commercial drugs[15]
caffeine	1.23	1351	v. high	v. high	101.8	1400	63.88	8.04	2/SWV	cola, tea, coffee[16]
theophylline	3.0	1170	90	11.0	192.6	2860	5.95	1.218	0.1/SWV	commercial drugs and tea[18]
codeine	1.1	1007	v. high	v. high					0.14/FIA	human plasma, drugs[17]
dopamine	7.0	250	100	+2.5	64.9	3000	1.849	0.455	0.1/SWV[10]	
serotonin	7.4	360	20	+6.0	810.2				0.002/SWV	human blood[11]
adenine	3.0	920	130	+20.5	138.5	600	0.450	0.101	0.02/SWV	DNA, RNA[12]
guanine	4.5	1110	150	+9.0	40.7	187	0.152	0.111	0.005/SWV	DNA, RNA[12]
cysteine	7.4	630	v. high	v. high	54.1	50000	131.4	6.330	1.7 nM/FIA[29]	biological proteins
hypoxanthine	9.0	911	80	+12.5	324.9	1200	1.191	15.02	0.75/SWV	aging of dead fishes[14]
xanthine	6.0	778	90	+2.4	254.9	1000	0.479	0.167	0.04/SWV	urine
uric acid	1.1	695	150	+3.2	58.5	1500	2.301	0.365	0.11/SWV	urine, serum[9]

[a] Current function. [b] CV at scan rate = 10 mV/s; v. high = very high; $I_{mag} = (i_{pa})_{NPyCME}/(i_{pa})_{GCE}$; D_L = detection limit.

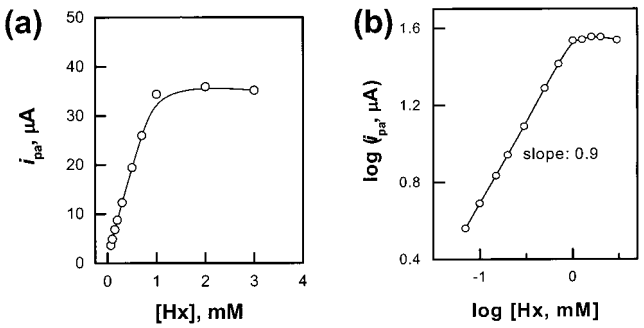

FIGURE 2. (a) The i_{pa} vs [Hx] plot for the CV responses of the NPyCME in 0−3 mM Hx in pH 9.0 ammonia buffer solution (v = 10 mV/s). (b) The log i_{pa} vs log [Hx] plot.

some standard redox couples on carbon electrodes were proved to resemble the *outersphere* model.[23] Instead, most organic and other biological compound oxidation reactions on the NPyCME showed a marked decrease (i.e., η) in oxidation potential together with a considerable increase in current magnitude ($I_{mag} = (i_{pa})_{NPyCME}/(i_{pa})_{GCE}$) over the results on the GCE (Table 2). It is expected that the electrocatalytic system operates through the formation of a precursor intermediate complex between the analyte and the catalytic site before product formation. Some of the functional group that is active to the catalytic site may help to bridge the analyte with the catalyst. This situation is quite similar to an *innersphere* electron-transfer model.[36] Electrocatalytic oxidation with increasing analyte concentration on the NPyCME showed saturation at a particular concentration (C_L in Table 2). For example, Hx reached the C_L value at 1200 μM under quasi-steady-state conditions (Figure 2).[14] The reaction order (m), i.e., (∂ log i_{pa}/∂ log C), measured is close to unity up to this C_L, and beyond that it is zero. This behavior is similar to the enzyme kinetics in many biological systems with a key-lock type catalyst/substrate complex high-energy intermediate and is expected to follow the *innersphere* electron-transfer mechanism.[19,31]

In addition to following the Michaelis−Menten kinetics behavior, the NPyCME mimics the enzyme in fine site mapping and can thus be considered as an enzyme analogue. Since the surrounding polymer can form the so-called polymeric field, the hydrophobic Nafion core/shell plays an important role not only in stabilization of the Py site, but also in the catalysis.[37] This situation is quite similar to that of an enzyme, where an active site is surrounded by protein. This protein can form a specific field, which fits to the corresponding substrate. Similarly, interaction between the surrounding polymers and reactive substrates can affect the activity and selectivity of the NPyCME.

The fundamental characteristic of the Michaelis−Menten mechanism is a transition from first-order to zero-order kinetics near a critical substrate concentration.[19,31] These results suggest the operation of the Michaelis−Menten mechanism type kinetics on the NPyCME. Other possibilities, such as adsorption of the electroactive compound, formation of dimeric species at high concentrations or complexation with the solvent, and association−dissociation chemistry at different concentrations, may also lead the current to reach a plateau at high concentrations. However, the perfect diffusion-controlled behavior of the NPyCME (i.e., ∂ log i_{pa}/∂ log $v \cong 0.5$) together with the fact that the molar absorption coefficient (ϵ) does not change upon increasing the analyst concentration disproves the above three factors.[8] Although this kinetics is well-known in enzymes and immobilized enzyme electrodes, there are very few reports of it in nonenzymatic sensors.[31,38]

Lyons et al. recently reported a theoretical model for the Michaelis−Menten analysis of microheterogeneous systems dispersed uniformly in a supporting matrix like Nafion.[31] The electrochemical equivalent of the Michaelis−Menten equation in terms of i_{pa} for Hx oxidation can be written as follows:

$$i_{pa} = \frac{nFAk_c\Gamma_t[\mathrm{Hx}]}{K_m + [\mathrm{Hx}]} = \frac{i_m[\mathrm{Hx}]}{K_m + [\mathrm{Hx}]} \qquad (1)$$

where $i_m = nFAk_c\Gamma_t$, Γ_t represents the total surface concentration of the electroactive ruthenium species and is obtained from the charge ($q = nFA\Gamma_t$) associated with redox transformation, k_c represents the first-order catalytic

Scheme 3. Electrocatalytic Mediated Mechanism for the Hypoxathine (Hx) Oxidation on the NPyCME: (a) Illustration of the Participation of the Ru(IV)/Ru(VI) Redox Sites in the Mediated Mechanism and (b) Reaction Pathway Based on the Michaelis−Menten Kinetics

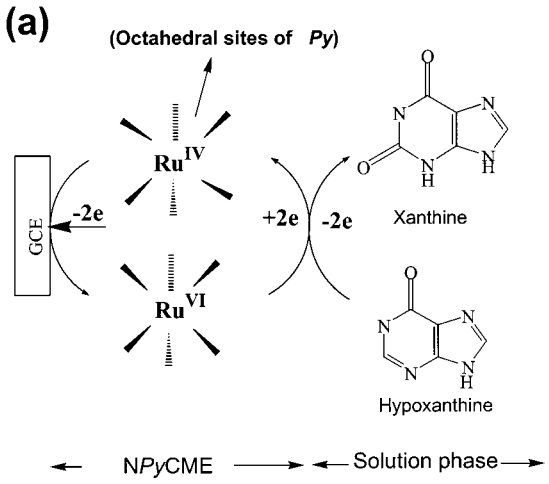

(b)

$$\text{Hx} + \textit{Py}\text{-Ru(VI)} \underset{}{\overset{K_m}{\rightleftharpoons}} [\text{Hx-}\textit{Py}\text{-Ru(VI)}] \xrightarrow[\text{(rds)}]{k_c} \textit{Py}\text{-Ru(IV)} + \text{X}$$

$$\textit{Py}\text{-Ru(IV)} \xrightarrow{k'_{ME}} \textit{Py}\text{-Ru(VI)} + 2e$$

rate constant for the decomposition of the catalyst/substrate intermediate to product, K_m is the Michaelis−Menten binding constant related to the equilibrium step of the product with catalyst/substrate intermediate, and other factors have their usual meaning. The calculation from curve fitting, Lineweaver−Burk (LB), and Eadie−Hofsee (EH) analysis were discussed in more detail in our recent report.[14] Table 2 also summarizes the kinetics information collected on the NPyCME from LB analysis. Scheme 3 represents a model example of the electrocatalytic mechanism for Hx oxidation on the NPyCME, where surface-bound Py-[Ru(IV)/Ru(VI)] is involved in the catalytic oxidation. The [Hx-Py-Ru(VI)] represents an intermediate and high-energy mimicking enzyme/substrate complex of the *innersphere* precursor formed by productive binding of the subtract on the active site. Decomposition of the above precursor is considered a rate-determining step (rds) for the overall Michaelis−Menten mechanism. The polymeric field of the hydrophobic core/shell contributes in a certain way to the productive binding and thus enhances the electron-transfer rate. In other words, the NPyCME represents a mimicking enzyme analogue.

Practical Applications

What is needed primarily for analytical application is quantitatively measurable and sharp peaks with good signal-to-noise ratio. Square-wave voltammetry (SWV) and flow injection analysis (FIA) are considered to be sensitive analytical tools for improving detecting-current signals.[39−41] The FIA was performed using the chronoamperometric ($i-t$) mode at a fixed potential (where the analyte is active

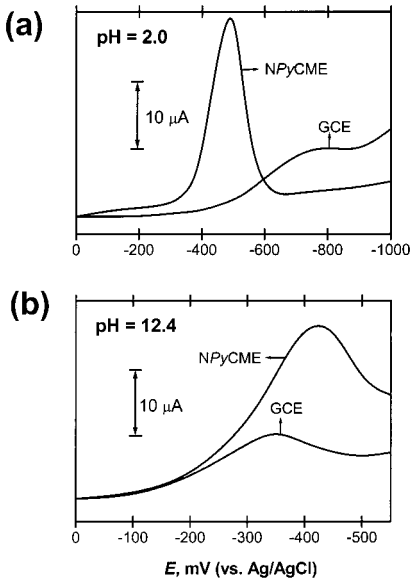

Dissolved oxygen (DO) measurements in water samples.

Sample	YSI DO meter $[O_2]$/ppm	NPyCME $[O_2]$/ppm	Relative error[a] (%)
Doubly deionized water	5.35	5.38	+0.56 (pH 2.0)
	6.90	6.99	+1.30 (pH 12.4)
Groundwater	6.87	6.78	-1.31 (pH 2.0)
	7.86	7.44	-5.34 (pH 12.4)

[a]Take the DO value measured by YSI DO meter as standard

FIGURE 3. Determination of dissolved oxygen at the NPyCME and bare GCE. SW voltammograms obtained in pH 2 solution (a) and pH 12.4 solution (b). Summarized at the bottom are results of dissolved oxygen measurement for different water samples.

to the NPyCME) under hydrodynamic flow of the base electrolyte. Usually, the volume of analyte used in FIA is ≤200 μL. The analytical applications using the above sensitive techniques on the NPyCME in various fields are reviewed below. Details of the literature comparison and optimization can be obtained from the respective references.

Environmental. Figure 3 shows the response of the NPyCME against dissolved oxygen in acidic and alkaline environments by SWV.[6] Compared to the response at GCE, a well-defined and sharp signal with ~250 mV decrease in overpotential and 5.2 times increase in peak signal was observed in pH 2 solution at the NPyCME. It is well-known that RuO_2 is not an efficient electrode material for the oxygen reduction reaction.[4,34] This is indeed another unique property and obvious advantage of the NPyCME, where the interstitially active O′ species existing in the Py network is responsible for the catalytic reaction.[3−6,34] Using this electrode, the detection range was found to lie between 0.7 and 8.4 ppm O_2. To confirm the accuracy of the method, two natural water samples were analyzed simultaneously using the NPyCME and a commercial YSI dissolved oxygen meter, and the results are finally rechecked with the standard Winkler's method, as shown in the table in Figure 3.[6] The results obtained on the

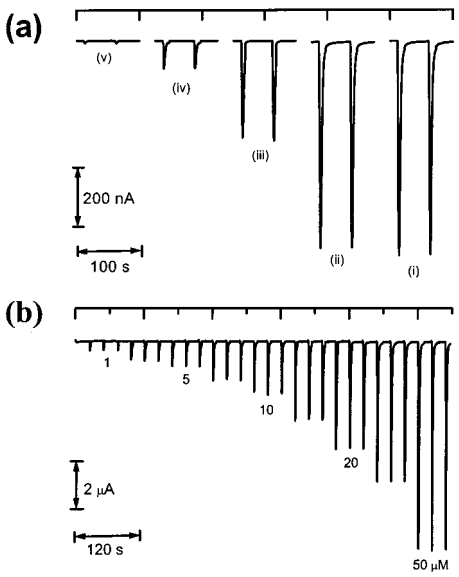

FIGURE 4. FIA of hydrazine and amitrole using the NPyCME. (a) FIA responses for (i) 10 μM hydrazine containing 100 μM oxalic acid, (ii) after addition of 50 ppm gelatin and 50 ppm albumin to (i), and (iii)−(v) same as (i) with decreasing hydrazine concentrations of 5, 1, and 0 μM at the NPyCME in pH 8.0 ammonia buffer solution. (b) FIA response of increasing concentration of amitrole in pH 3.6 $HClO_4$/$NaClO_4$ solution. Flow rate was 1.0 mL/min with an applied potential of 0.7 V vs Ag/AgCl for (a) and 1.2 V for (b).

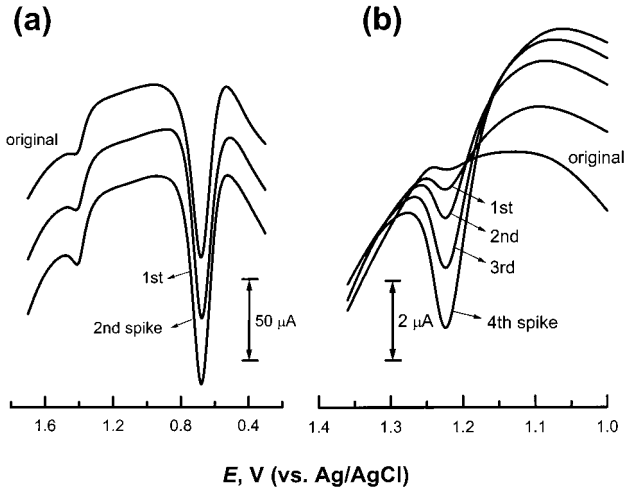

FIGURE 5. Determination of acetaminophen, caffeine, and theophylline using the NPyCME. (a) SWV responses for simultaneous determination of acetaminophen and caffeine in commercial available drug with 10 μM concentration of the above compounds per spike. (b) Theophylline determination in green tea with spiking concentration of 20 μM for four successive spikes in pH 3 phosphate solution.

NPyCME were very close to those obtained with an oxygen meter and were also in good agreement with results obtained with classical procedures.

To eliminate the interference of oxalic acid on the detection assays of the industrially and pharmacologically important hydrazine is a practical target. Cobalt phthalocyanine (CoPC)/Nafion CME is considered to be a good electrode to solve this problem through CoPC's mediation and Nafion's permselective rejection of oxalate anions on the surface.[42] Nevertheless, the surface poisoning of this electrode due to other interferences such as gelatin and albumin cannot be prevented. Such interference, however, is negligible during the hydrazine assay on the NPyCME in pH 8.0 ammonia buffer solution, as shown in Figure 4a. The D_L value is 0.15 μM (S/N = 3), i.e., 0.048 ng in 20 μL sample by FIA. A similar procedure was further developed for amitrole detection (Figure 4b), which is widely used as a herbicide along roads and railway tracks and in agriculture as mixed formulations with other pesticides.[8] The amitrole content in drinking water was monitored at a regulatory level of 0.1 μg/L in European countries. A D_L of 0.15 ng in a 20 μL sample was obtained by FIA, giving an easy route to monitor amitrole in real systems.

Pharmaceutical and Food. Acetaminophen is a widely used analgesic anti-pyretic drug often formulated with caffeine, which is a stimulant to the central nervous and cardiovascular systems. Simultaneous determination of the above formulation is a challenge in the pharmaceutical assays. Figure 5a shows the simultaneous determination of acetaminophen and caffeine in commercially available drugs using the NPyCME in 0.05 M perchloric acid solution.[15] The NPyCME can also be extended to food analysis for caffeine in beverages such as cola, coffee, and tea with good sensitivity and selectivity.[16] Theophylline is a xanthine derivative, another cardiac stimulant drug and smooth-muscle relaxant; it is also used for the treatment of asthma.[18] The use of the NPyCME in the measurement of theophylline-containing samples such as ampule, tablet, black tea, and green tea (Figure 5b) is also very promising.

Evaluation of the freshness of fish is an unresolved problem in food testing processes. It is normally pursued from the detection assay of Hx released after the death of the animals. This is a typical class of aging index studies. Normally, the Hx monitoring electrodes were constructed using the xanthine oxidase (XOD) enzyme. Unfortunately, XOD is not specific toward Hx alone; it also reacts with xanthine, making the detection system more complicated.[14] The NPyCME, however, can sense Hx alone through the electrocatalytic effect and has been successfully applied to monitor the freshness of two kinds of locally available fish, namely *Carassius aurathus* and *Tilapia mossambia*. The Hx contents monitored by the NPyCME for fish samples 1, 24, and 48 h after death are 0.48, 2.80, and 8.76 μmol/g, respectively. A similar trend was also noticed for different fish and has clearly demonstrated that Hx release is directly related to the decreasing freshness of fish. We also investigated the simultaneous determination of Hx, xanthine, and uric acid on NPyCME as shown in Figure 6.[9,14] This result can open more quantitative applications in biomedias.

Biomedical. Dopamine and serotonin are important neurotransmitters that are active in the control and regulation of brain function. The main problem with GCE in the detection assays is the interference from ascorbic acid (AA) due to the overlap of oxidation potentials. A regular level of dopamine in biological systems is 0.01−1

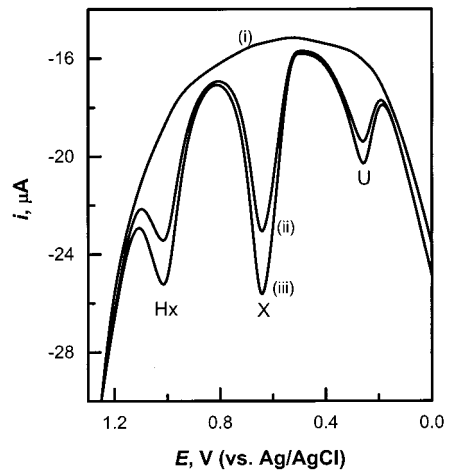

FIGURE 6. Simultaneous determination of uric acid (U), xanthine (X), and hypoxanthine (Hx) using the NPyCME. SWV responses for (i) 0, (ii) 20, and (iii) 30 μM concentration of U, X, and Hx, respectively, in pH 7 phosphate buffer solution.

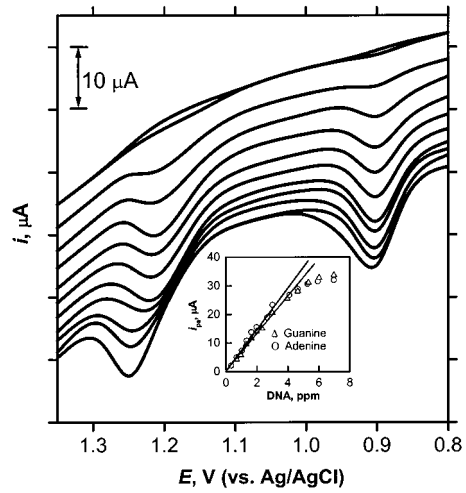

FIGURE 7. Simultaneous determination of guanine and adenine in DNA with increasing concentration of 0.33−3.96 ppm at 0.33 ppm intervals in pH 4.0 solution at the NPyCME.

μM, and the concentration of AA is much higher (~0.1 mM) than that of dopamine. Since AA is insensitive on the NPyCME, the interference can easily be eliminated. The calculated D_L is 0.1 μM, with a preconcentration time of 60 s at a preconcentration potential of −0.3 V vs Ag/AgCl.[10] With regard to serotonin, the D_L is 2 nM in pH 9.0 ammonia buffer solution and was successfully applied to the serotonin analysis in human blood samples.[11]

Chemical sensors for the simultaneous quantification of purine bases such as guanine (G) and adenine (A) in nucleic acid have been developed on the NPyCME by SWV (Figure 7).[12] The detection limits for G and A were 11.5 and 37.7 ng/mL, respectively. Assayed G and A values for synthetic oligonucleotides, D55 (5′GCGGTACAAAATGGGCGC3′) and BR2 (5′GTGCAATGCAATGCAAC3′), and some nucleic acids, like calf thymus DNA and yeast RNA, were all in good agreement with spectroscopic results.

The NPyCME can also be extended to the dual electrocatalytic reactions of NO_2^- oxidation and NO reduction

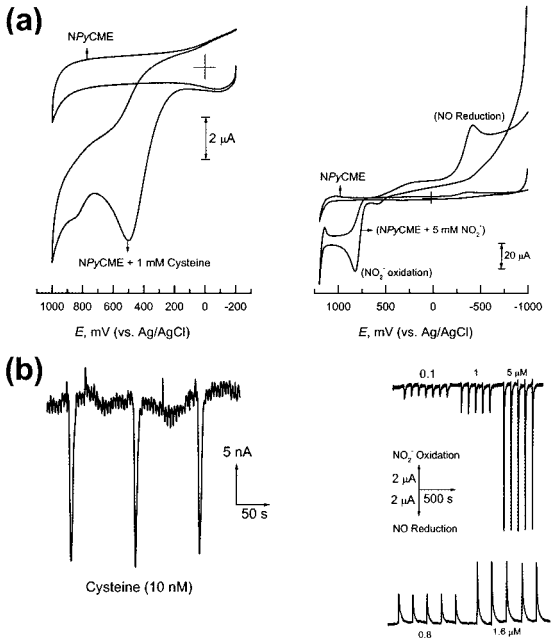

FIGURE 8. Determination of cysteine, NO_2^-, and NO using the NPyCME. (a) CV responses for cysteine (v = 50 mV/s) in pH 7.4 solution and for NO_2^- oxidation and NO reduction (v = 5 mV/s) in pH 1.65 KCl solution. (b) FIA responses for cysteine (flow rate = 0.3 mL/min at 1.0 V vs Ag/AgCl), NO_2^- (flow rate = 0.3 mL/min at 1.1 V vs Ag/AgCl), and NO (flow rate = 0.5 mL/min at −0.8 V vs Ag/AgCl).

(Figure 8).[43] These are also important constituents in biological media; their simultaneous measurements is believed to be a real challenge. The NPyCME provides a detection range of 100 nM−100 μM and 800 nM−63.3 μM and a D_L of 4.8 and 15.6 nM for NO_2^- and NO, respectively.

All the above analyses prove the ideality and success of this novel NPyCME for real systems. Moreover, the NPyCME showed good long-term stability, as no decreases in peak signals were observed after the electrode was stored in 1 M KOH solution for more than 3 months. Unlike the surface poisoning effect from halides, S^{2-}, surfactant, etc. and corrosive behavior due to high acid and alkaline pH values on conventional electrodes, these effects are not so operative on the NPyCME due to a network with rigid polymeric backbones.

Future and Perspective

(i) Analysis of protein folding/defolding is also a possible goal in developing the NPyCME. Recent FIA measurements on cysteine (R−SH) showed a sharp and obvious response for the 10 nM sample with a D_L of 1.7 nM in pH 7.4 buffer (Figure 8).[29] This is one of the lowest values ever reported. Thus, by coupling the NPyCME with real protein samples, one can certainly get information about the −SH (i.e., cleaved disulfides) quantification and in turn about the analysis mentioned above. Note that the NPyCME is specific to R−SH oxidation alone and not for RS−SR reduction. At neutral pH, the FIA signals are not altered with respect to other biological interferences like disulfides, sulfonic acid, glucose, and ascorbic acid.

Scheme 4. Photochemical Oxidation Reaction on the $Ru(bpy)_3^{2+}$/ Py-Doped Nafion Membrane

Experimental Setup

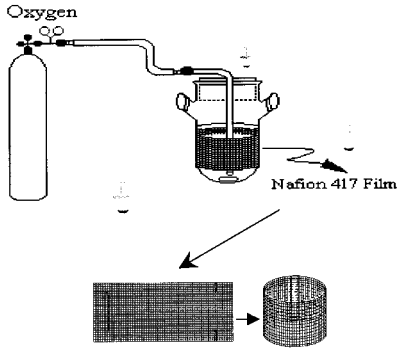

Nafion 417 film

Mechanism for the photochemical oxidation of anisole

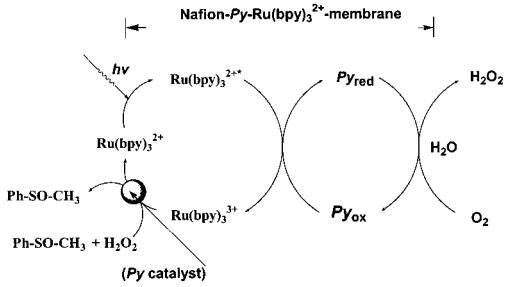

(ii) The NPyCME is promising for other, newer biological systems that contain functional groups like −OH, −SH, etc.

(iii) The preparation of Py units in other cationic-exchange matrixes like clay can also lead to the birth of another class of chemical sensor.

(iv) The NPyCME can also be prepared as a disposable screen-printed electrode and is more suitable for real samples and commercial use.

(v) As a new approach, we have coupled this in situ precipitation technique for application in synthetic photoorganic chemistry. The Py units were first precipitated (partially) directly in a Nafion membrane followed by ion exchange of a photosensitizer like $Ru(bpy)_3^{2+}$, and this multicomponent film showed efficient catalytic effect in selective oxidation of thioanisole ($Ph-S-CH_3$). This model system in the presence of aqueous acetonitrile, H^+, O_2, and under the illumination of a 500-W halogen lamp for 12 h resulted in more than 90% yield of $Ph-SO-CH_3$ (Scheme 4).

(vi) Since the Py units are derived from precious metallic oxide groups, one can further extend their application to other research fields like photoassisted splitting of water, solar energy conversion, etc.

Overall, this new NPyCME has a wide scope in the diverse research fields of material science, electrocatalysis, chemical and biochemical sensors, and photoorganic synthetic chemistry. Numerous applications can readily be imagined from the NPyCME discussed above.

Glossary

Py	lead−ruthenium oxide pyrochlore
NPyCME	Nafion/lead−ruthenium oxide pyrochlore chemically modified electrode
NPyCE	Nafion + Py powder composite electrode
GCE	glassy carbon electrode
v	scan rate
ΔE_p	peak potential separation
i_{pa}	anodic peak current
i_{pc}	cathodic peak current
i_f	current function
k^o	heterogeneous electron transfer rate constant
ψ	kinetic parameter
D_o	diffusion coefficient of the oxidant
D_R	diffusion coefficient of the reductant
n	total number of electron
F	Faraday's constant
R	gas constant
SWV	square-wave voltammetry
FIA	flow injection analysis
m	order of reaction
T	temperature
α	transfer coefficient
η	overpotential
$\Delta H^{\#}$	enthalpy of activation
I_{mag}	current magnitude
C	concentration of analyte
C_L	saturation concentration
D_L	detection limit
Γ_t	surface concentration of the electroactive species
A	electrode area
q	surface charge
K_m	Michaelis−Menten binding constant
k_c	catalytic rate constant
k'_{ME}	electrochemical rate constant
Hx	hypoxanthine

During his nine years at NCHU, J.-M.Z. has been privileged to work with many enthusiastic co-workers. The authors gratefully acknowledge financial support from National Science Council of the Republic of China.

References

(1) Trasatti, S. Transition Metal Oxide-Electrocatalysis. In *Electrochemistry of Novel Materials*; Lipkowski, J., Ross, P. N., Eds.; VCH Publication, Inc.: New York, 1994; Chapter 5.
(2) Ricco, A. J.; Crooks, R. M. Chemical Sensors−Editorial View. *Acc. Chem. Res.* **1998**, *35*, 200.
(3) Goodenough, J. B.; Manoharan, R.; Paranthaman, M. Surface Protonation and Electrochemical Activity of Oxides in Aqueous Solution. *J. Am. Chem. Soc.* **1990**, *112*, 2076−2082.
(4) Zen, J.-M.; Manoharan, R.; Goodenough, J. B. Oxygen Reduction on Ru−Oxide Pyrochlores Bonded to a Proton-Exchange Membrane. *J. Appl. Electrochem.* **1992**, *22*, 140−150.
(5) Zen, J.-M.; Wang, C.-B. Oxygen Reduction on Ruthenium-Oxide Pyrochlore Produced in a Proton-Exchange Membrane. *J. Electrochem. Soc.* **1994**, *141*, L51−L52.
(6) Zen, J.-M.; Wang, C.-B. Determination of Dissolved Oxygen by Catalytic Reduction on a Nafion/Ruthenium-Oxide Pyrochlore Chemically Modified Electrode. *J. Electroanal. Chem.* **1994**, *368*, 251−256.
(7) Zen, J.-M.; Tang, J.-S. Flow Injection Amperometric Detection of Hydrazine by Electrocatalytic Oxidation at a Perfluorosulfonated Ionomer/Ruthenium Oxide Pyrochlore Chemically Modified Electrode. *Anal. Chem.* **1995**, *67*, 208−211.
(8) Zen, J.-M.; Senthil Kumar, A.; Chang, M.-R. Electrocatalytic Oxidation and Trace Detection of Amitrole Using a Nafion/Lead−Ruthenium Oxide Pyrochlore Chemically Modified Electrode. *Electrochim. Acta* **2000**, *45*, 1691−1699.
(9) Zen, J.-M.; Tang. J.-S. Square-Wave Voltammetric Determination of Uric Acid by Catalytic Oxidation at a Perfluorosulfonated Ionomer/Ruthenium Oxide Pyrochlore Chemically Modified Electrode. *Anal. Chem.* **1995**, *67*, 1892−1895.

(10) Zen, J.-M.; Chen, I-L. Voltammetric Determination of Dopamine in the Presence of Ascorbic Acid at a Chemically Modified Electrode. *Electroanalysis* **1997**, *9*, 537−540.
(11) Zen, J.-M.; Chen, I-L.; Shih, Y. Voltammetric Determination of Serotonin in Human Blood Using a Chemically Modified Electrode. *Anal. Chim. Acta* **1998**, *369*, 103−108.
(12) Zen, J.-M.; Chang, M.-R.; Ilangovan, G. Simultaneous Determination of Guanine and Adenine Contents in DNA, RNA and Synthetic Oligonucleotides Using a Chemically Modified Electrode. *Analyst* **1999**, *124*, 679−684.
(13) Zen, J.-M.; Senthil Kumar, A.; Chen J.-C. Electrocatalytic Oxidation of Cysteine on a Nafion-Ruthenium Oxide Pyrochlore Chemically Modified Electrode. *Chem. Lett.* **1999**, 743−744.
(14) Zen, J.-M.; Lai, Y.-Y.; Ilangovan, G.; Senthil Kumar, A. Electrocatalytic Oxidation of Hypoxanthine on a Nafion/Lead−Ruthenium Oxide Pyrochlore Modified Electrode. *Electroanalysis* **2000**, *12*, 280−286.
(15) Zen, J.-M.; Ting, Y.-S. Simultaneous Determination of Caffeine and Acetaminophen in Drug Formulations by Square-Wave Voltammetry Using a Chemically Modified Electrode. *Anal. Chim. Acta* **1997**, *342*, 175−180.
(16) Zen, J.-M.; Ting, Y.-S.; Shih, Y. Voltammetric Determination of Caffeine in Beverages Using a Chemically Modified Electrode. *Analyst* **1998**, *123*, 1145−1147.
(17) Zen, J.-M.; Chang, M.-R.; Chung, H.-H.; Shih, Y. Determination of Codeine in Human Plasma and Drug Formulation Using a Chemically Modified Electrode. *Electroanalysis* **1998**, *10*, 536−540.
(18) Zen, J.-M.; Yu, T.-Y.; Shih, Y. Determination of Theophylline in Tea and Drug Formulation Using a Nafion/Lead−Ruthenium Oxide Pyrochlore Chemically Modified Electrode. *Talanta* **1999**, *50*, 635−640.
(19) Voet, D.; Voet, J. G. *Biochemistry*, 2nd ed.; John Wiley & Sons: New York, 1995; Chapter 13, pp 345−370.
(20) Yeo, R. S.; Yeager, H. L. Structural and Transport Properties of Perfluorinated Ion-Exchange Membranes. In *Modern Aspects of Electrochemistry*; Conway, B. E., White, R. E., Bockris, J. O'M., Eds.; Plenum Press: New York, 1985; Chapter 6.
(21) Horowitz, H. S.; Longo, J. M.; Lewandowski, J. T. Electrochemical Device Having an Oxygen Electrode Containing a Pyrochlore Type Compound Electrocatalyst. U.S. Patent 4,129,525, 1978.
(22) Longo, J. M.; Raccah, P. M.; Goodenough, J. B. Preparation and Properties of Oxygen Deficient Pyrochlore. *Mater. Res. Bull.* **1969**, *4*, 191−202.
(23) Deakin, M. R.; Stutts, K. J.; Wightman, R. M. The Effect of pH on Some Outer-Sphere Electrode Reactions at Carbon Electrodes. *J. Electroanal. Chem.* **1985**, *182*, 113−122.
(24) Nicholson, R. S. Theory and Application of Cyclic Voltammetry for Measurement of Electrode Reaction Kinetics. *Anal. Chem.* **1965**, *37*, 1351−1355.
(25) Kawiak, J.; Jedral, T.; Galus, Z. Reconsideration of the Kinetic Data for the $Fe(CN)_6^{3-/4-}$ System. *J. Electroanal. Chem.* **1983**, *145*, 163−171.
(26) Kawiak, J.; Jedral, T.; Galus, Z. A Search for Conditions Permitting Model Behavior of the $Fe(CN)_6^{3-/4-}$ Redox System. *J. Electroanal. Chem.* **1987**, *226*, 305−314.
(27) Chandrasekara Pillai, K.; Thangamuthu, R.; Ilangovan, G. Dependence of Pt Pretreatment Effect on $Fe(CN)_6^{3-/4-}$. *Electroanalysis* **1995**, *12*, 1182−1188.
(28) Hanania, G.; Irvine, D. H.; Eaton, W. A.; George, P. Thermodynamic Aspects of Potassium Hexacyanoferrate(III)-(II)-Reduction Potentials. *J. Phys. Chem.* **1967**, *71*, 2022−2030.
(29) Zen, J.-M.; Senthil Kumar, A.; Chen, J.-C. Electrocatalytic Oxidation and Sensitive Detection of Cysteine on a Lead Ruthenate Pyrochlore Modified Electrode. *Anal. Chem.* **2001**, *73*, 1169−1175.
(30) Burke, L. D.; Healy, J. F. The Importance of Reactive Surface Groups for RuO_2 Redox Transitions, *J. Electroanal. Chem.* **1981**, *124*, 327−332.
(31) Lyons, M. E. G. Transport and Kinetics in Electroactive Polymers. In *Advances in Chemical Physics Polymeric Systems*; Prigogine, I., Rice, S. A., Eds.; John Wiley & Sons: New York, 1996; pp 297−624.
(32) Senthil Kumar, A.; Chandrasekara Pillai, K. Studies of Electrochemical Behaviour of RuO_2−PVC film Electrodes: Dependence on Oxide Preparation Temperature. *J. Solid State Electrochem.* **2000**, *4*, 408−416.
(33) Because the ruthenium redox potentials are pH-dependent, to compare the reported standard redox potential of ruthenium metal ions in the reversible hydrogen scale (RHE, where $E^o_{RHE} = 0$ V), the simplified equation $E_{RHE} = [(E_{Ag/AgCl} + 0.075pH) + E^o_{Ag/AgCl}]$ is used to adjust the potentials from $E_{Ag/AgCl}$ to E_{RHE}.
(34) Zen, J.-M.; Senthil Kumar, A.; Chen, J.-C. Electrochemical Behavior of Lead−Ruthenium oxide Pyrochlore Catalyst: Redox Characteristics in Comparison with that of Ruthenium dioxide. *J. Mol. Catal. A* **2001**, *165*, 177−188.
(35) Savinell, R. F.; Zeller, R. L.; Adams, J. A. Electrochemically Active Surface Area. *J. Electrochem. Soc.* **1990**, *137*, 489−494.
(36) Purcell, K. P.; Kotz, J. C. *Inorganic chemistry*; W. B. Saunders Co.: Philadelphia, 1977; Chapter 12, pp 654−693.
(37) Toshima, N. Nanostructured Metal Clusters in Polymeric Field as a Model of Artificial Enzyme. *Supramol. Sci.* **1998**, *5*, 395−398.
(38) DaSilva, M. F. C. G.; DaSilva, J. A. L.; DaSilva, J. J. R. F.; Pombeiro, A. J. L.; Amatore, C.; Verpeaux, J. N. Michaelis−Menten Type Mechanism in the Electrocatalytic Oxidation of Mercaptopropionic Acid by Vanadium Complex. *J. Am. Chem. Soc.* **1996**, *118*, 7568−7573.
(39) Osteryoung, J. G.; Osteryoung, R. A. Square Wave Voltammetry. *Anal. Chem.* **1985**, *57*, 101A−110A.
(40) Lovric, S. K.; Lovirc, M.; Bond, A. M. Square-Wave Stripping Voltammetry of Lead and Mercury. *Anal. Chim. Acta* **1992**, *258*, 299−305.
(41) Wang, J. *Analytical Electrochemistry*; VCH Publishers: New York, 1994; pp 54−64.
(42) Wang, J.; Li, R. Multifunctional Chemically Modified Electrodes with Mixed Cobalt Phthalo-Cyanine/Nafion Coatings. *Talanta* **1989**, *36*, 279−284.
(43) Zen, J.-M.; Senthil Kumar, A.; Wang, H.-F. A Dual Electrochemical Sensor for Nitrite and Nitric Oxide. *Analyst* **2000**, *125*, 2169−2172.

AR000073N